XXII SITRAER 2025
Simpósio de Transporte Aéreo

FMS OPTIMUM VERTICAL AND LATERAL TRACKING FOR REDUCED FUEL CONSUMPTION

Lucas Cardoso Navarro[1], Luiz Carlos Sandoval Góes[1], José Alexandre Tavares Guerreiro Fregnani[1]
1. Instituto Tecnológico de Aeronáutica
*** Corresponding author e-mail address**: lucas_sertao@hotmail.com / luiz.goes@gp.ita.br / eng.fregnani@hotmail.com

ABSTRACT

This study addresses the optimization of flight paths in specific airspaces that permit aircraft to navigate along flexible lateral routes between designated entry and exit points, such as those found in the South Atlantic, Indian Ocean, and Pacific Ocean. Current flight planning systems typically optimize trajectories by calculating great-circle routes between selected waypoints, focusing on minimizing flight costs. However, these systems often lack the capability to adjust the flight path direction dynamically to reduce the impact of headwinds. To address this limitation, we propose an innovative algorithm for the Flight Management System (FMS) aimed at decreasing overall fuel consumption during flight. This algorithm allows for modifications to both lateral and vertical flight paths within a defined range, effectively minimizing the influence of direct wind components. By doing so, it offers a more fuel-efficient alternative compared to traditional direct routing between origin and destination points. For proof of concept, we developed a Simulink model that simulates the aircraft dynamics, autopilot control algorithms, and atmospheric conditions across various scenarios. The results indicate that the proposed algorithm can achieve fuel consumption reductions of up to 2% in certain flight conditions. Furthermore, this algorithm has the potential to be incorporated into the Boeing Flight Management System (BFMS) as an uplink feature.

Keywords: Flight Management System (FMS), Fuel Consumption, Trajectory Optimization, Headwind Minimization, Modeling.

GENERATIVE AI USAGE STATEMENT

This research did not use generative AI.

FMS OPTIMUM VERTICAL AND LATERAL TRACKING FOR REDUCED FUEL CONSUMPTION

1 INTRODUCTION

Certain airspaces around the world, such as the South Atlantic, Indian Ocean, and Pacific Ocean, are designed to allow aircraft to fly along various lateral paths between specific entry and exit gates at the borders of these areas. Figure 1 illustrates the so-called Atlantic Ocean Route for the Region of the Americas (AORRA). This airspace is characterized by its allowance for lateral deviations from traditional flight paths, enabling airlines to optimize routes based on real-time environmental conditions, such as wind patterns and weather phenomena. The flexibility inherent in AORRA is particularly beneficial for enhancing fuel efficiency, as it allows pilots to adjust their trajectories to minimize headwinds and maximize tailwinds, ultimately leading to reduced operational costs. This flexibility provides an opportunity to implement sophisticated algorithms capable of dynamically adjusting flight trajectories based on real-time wind data. By incorporating real-time meteorological data into the flight management system (FMS), the proposed algorithm aims to enhance the precision of trajectory optimization.

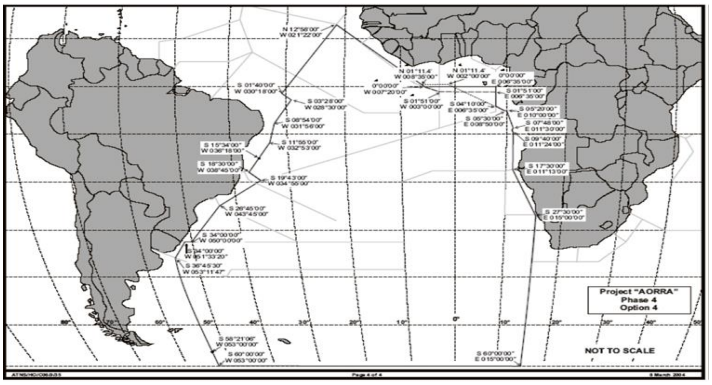

Figure 1: South Atlantic Random Routings (AORRA) (ICAO, 2011)

2 LITERATURE REVIEW

Airlines can significantly reduce fuel usage and travel duration by employing wind-optimal approaches instead of fixed flight paths. Various automated methods have been suggested to identify effective solutions, with a focus on discretizing the trajectory optimization problem and representing potential flight paths as graph diagrams. This framework allows for the application of greedy algorithms to find the shortest path, enhancing navigation in complex air traffic environments while minimizing fuel consumption.

For instance, Ma et al. (2025) propose a route planning framework that integrates wind field predictions from a neural network, focusing on major airline routes over China. Ramee et al. (2020) create a grid using waypoints in the U.S. to gather weather information and calculate costs between nodes, although it does not optimize altitudes. Legrand et al. (2018) develop a 2D grid approach for trajectory prediction without vertical optimization.

Mendonza et al. (2014) utilize Dijkstra's algorithm for trajectory optimization, considering various parameters like aircraft weight and wind influence. Ng et al. (2014) separate route optimization into vertical and lateral components, focusing on lateral optimization with wind. Schilk and Hecker (2014) present a trajectory optimization system using real-time weather data, employing modified A* and Theta* algorithms to reduce detours and fuel consumption. Gagné et al. (2013) introduce an algorithm for optimizing flight trajectories using real-time meteorological data.

Knapp et al. (2008) develop the Aviation Weather Routing Tool (AWRT), which uses a 4-D grid of weather data to optimize flight paths with the A* algorithm, effectively minimizing adverse

weather impacts. Wickramasinghe et al. (2012) create a 4-D optimal flight trajectory model that integrates aircraft performance and meteorological forecasts, focusing on fuel consumption through Dynamic Programming optimization.

Dai et al. (2024) formulates a 3-D propulsion energy consumption model for rotary-wing UAVs, addressing wind disturbances to enhance energy efficiency. Singh (2017) employs a genetic algorithm for optimizing fuel consumption in three-dimensional flight planning. Patrón et al. (2014a, 2014b) analyze dual approaches to trajectory optimization, combining vertical and lateral navigation profiles to minimize fuel consumption.

Lastly, Huang et al. (2020) explore an improved ant colony optimization and A* algorithm for 3D track planning in electric power inspection, emphasizing minimal energy consumption.

Overall, the variations in methodologies stem from different graph construction techniques and optimization constraints, significantly impacting the effectiveness and efficiency of trajectory optimization results.

3 OBJECTIVE

The primary objective of this research is to develop an algorithm designed to optimize both vertical and lateral flight trajectories, with the intent of minimizing the headwind component and consequently reducing overall fuel consumption. Figure 2 illustrates an example of how the optimized lateral profile (black) would look like considering actual wind profiles in the AORRA airspace. A great circle route (magenta) is also displayed in the sake comparison.

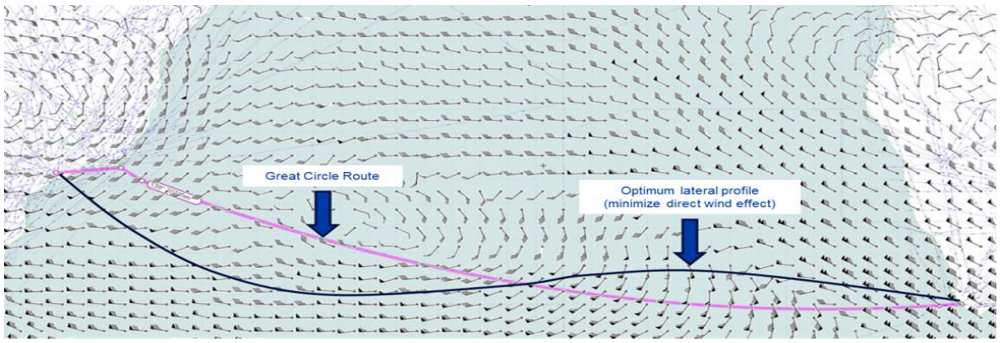

Figure 2: Optimized lateral profile.

4 METHODOLOGY

The proposed algorithm utilizes a grid-based approach to analyze potential flight paths. Each grid point is evaluated for wind speed and direction, allowing the algorithm to calculate the operational cost associated with each potential route. The algorithm is designed to construct a grid between the designated departure and arrival points, with each vertex of the grid representing a potential flight path. For each grid point, wind information is retrieved, enabling the algorithm to calculate both the distance and the associated cost for transitioning between nodes. With this information, it is possible to build a node diagram, making it easier to apply algorithms to find the shortest path. Figure 3 exemplifies a node diagram. With node diagrams, several techniques to calculate the optimal path are documented, well known as greedy algorithms. For the application of this work, the vertices of the grid are equivalent to the nodes, the edges are the paths between each vertex and the associated cost for transitioning between nodes is the weight.

A greedy algorithm is utilized to identify the optimal path by evaluating the distance and fuel cost for each segment of the flight. It considers the wind speeds and directions within a specified range, both vertically and horizontally, throughout the entire flight path. Using the geographic coordinates (longitude and latitude) of the aircraft's departure and arrival locations, the algorithm determines the ideal vertical and horizontal range for which wind information will be considered. Subsequently, within this defined range, a grid comprising (n) rows and (m) columns, the (n x m) grid is established. For each vertex within this grid, the algorithm retrieves the corresponding wind speed and direction, calculates the latitude and longitude, and determines the altitude, as depicted in Figure 4.

With the data collected from the grid, the algorithm can calculate both the distance and the cost for the aircraft to transition from one vertex to another.

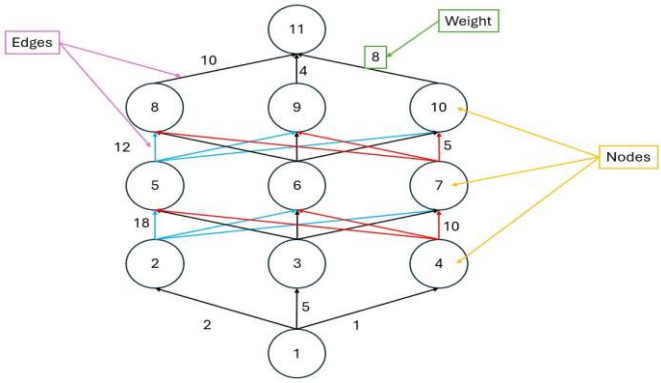

Figure 3: Example of Node Diagram.

To compute distances, the algorithm employs the indirect Vincenty algorithm (Vincenty,1975) and incorporates a slope factor to account for changes in altitude.

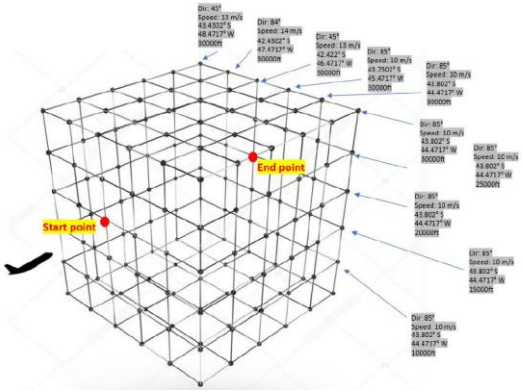

Figure 4: Grid built between the departure and arrival of the aircraft, populated with latitude, longitude, wind information and altitude.

It is posited that upon activation of the Autopilot system, the algorithm receives input data, including the endpoint coordinates (latitude and longitude), the number of rows and columns in the grid, and the permissible range for both horizontal and vertical flight paths. Subsequently, the algorithm initiates the calculation of distances and costs associated with all potential flight trajectories, thereby constructing a node diagram. The precision of the algorithm is directly proportional to the number of rows and columns in the grid; an increase in grid resolution enhances accuracy but also intensifies the computational load required to identify the optimal path. Figure 5 illustrates a three-dimensional representation of the grid utilized for the aircraft's trajectory.

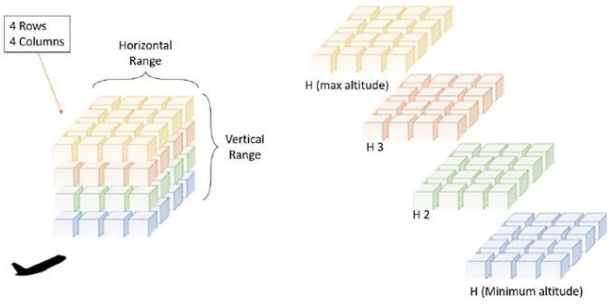

Figure 5: Altitude Grid.

Each cell within this cube corresponds to a node, with its respective longitude and latitude determined using the direct Vincenty formulas, along with an associated altitude. Upon establishing the grid, it is essential to associate each node with corresponding wind speed and direction data. This information can be obtained from online resources that provide real-time wind maps and forecasts, allowing for precise retrieval at specific longitude, latitude, and altitude coordinates. Following this, the subsequent step involves defining the paths or edges that connect each node within the grid. Each node will be linked to all adjacent nodes located in the subsequent row across all altitudes, as illustrated in Figure 6. In this example, each node has the potential to connect to 16 different paths.

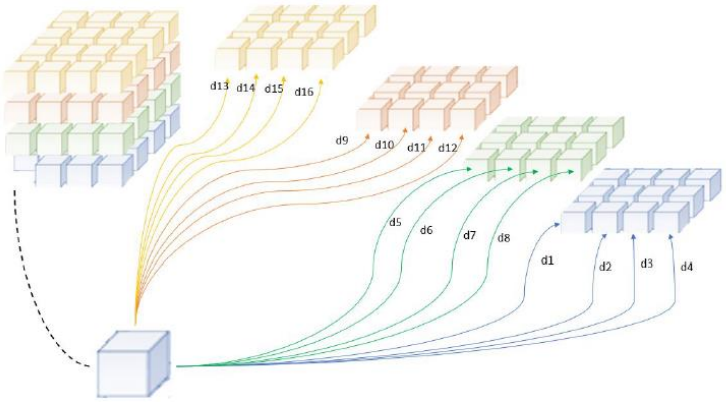

Figure 6: Paths between nodes.

The subsequent step involves calculating the distance and associated costs for each path or edge within the grid. Distances between nodes are determined using the indirect Vincenty equations, which are particularly effective for geodetic calculations. In instances where the nodes are situated at different altitudes, simple trigonometric methods are employed to ensure accurate distance measurements, as illustrated in Figure 7.

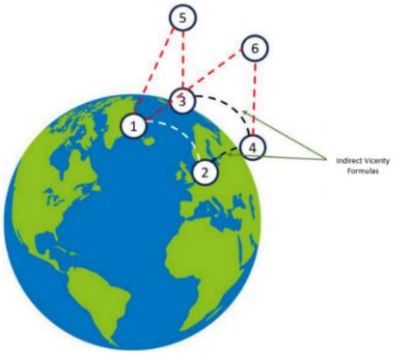

Figure 7: Distance Calculation between Nodes.

The operational cost associated with each potential flight path is determined by integrating the effects of wind speed and direction, which significantly influence the aircraft's ground speed and fuel consumption. The cost calculation encompasses both the time required and the amount of fuel necessary for the aircraft to transition from one vertex to another within the grid. Specifically, wind speed and direction are critical components of this cost assessment, as they directly affect the resultant speed of the aircraft. For instance, if the wind is oriented directly opposite the aircraft's trajectory between two analyzed vertices, this condition would result in a considerable reduction in the aircraft's ground speed. Consequently, the aircraft would incur increased fuel consumption and extended travel time for that segment of the flight, thereby raising the overall cost associated with that section. To ascertain the optimal flight path, a greedy algorithm is employed. In this framework, the vertices of the grid are represented as nodes, while the edges signify the paths connecting each vertex. The cost

calculated for each path functions as the weight in the algorithm's decision-making process, guiding the selection of the most efficient trajectory. To calculate the cost associated with each edge, the integration of the wind speed and the cost index is done. The cost function is derived from the definition of the aircraft costs.

$$cost = c_t * \Delta t + c_f * \Delta w_{fuel} \quad (1)$$

where c_t is the crew time cost (\$/seg), c_f is the fuel cost (\$/liter) and they are related by the cost index $CI = \frac{c_t}{c_f}$.

$$\Delta t = \frac{d}{V_{ground}} \; / \; \Delta w_{fuel} = \dot{m}_F * \Delta t \quad (2)$$

Replacing (2) in (1), results in:

$$cost = c_t * \frac{d}{V_{ground}} + c_f * \Delta t * \dot{m}_F \quad (3)$$

To derive the fuel flow formula ($\dot{m_F}$), the thrust required formula for climb phase is used:

$$T = D + W * \sin(\theta) \quad (4)$$

where:

$$D = \frac{1}{2} * \rho * S * V^2 * C_D \; / \; C_D = C_{D0} + k * {C_L}^2 \; / \; C_L = \frac{2*W}{\rho * S * V^2} \quad (5)$$

Replacing (5) in (4), and simplifying, results in:

$$T = \frac{1}{2} * \rho * S * V^2 * C_{D0} + \frac{k * 2 * W^2}{\rho * S * V^2} + W * \sin(\theta) \quad (6)$$

The fuel flow formula ($\dot{m_F}$) can be written as:

$$\dot{m}_F = T * TSFC \quad (7)$$

Replacing (6) in (7), results in:

$$\dot{m}_F = \left(\frac{1}{2} * \rho * S * V^2 * C_{D0} + \frac{k * 2 * W^2}{\rho * S * V^2} + W * \sin(\theta)\right) * TSFC \quad (8)$$

Thrust-Specific Fuel Consumption (TSFC) can be written as a linear equation:

$$TSFC = c_a * V + c_b \quad (9)$$

Replacing (9) in (8), results in:

$$\dot{m}_F = \left[\left(\frac{1}{2} * \rho(h) * S * V^2 * C_{D0}\right) + \left(\frac{k * 2 * W^2}{\rho(h) * S * V^2}\right) + (W * \sin(\theta))\right] * (c_a * V + c_b) \quad (10)$$

Replacing (10) in (3), results in:

$$Cost = \frac{d}{V_{ground}} * \left(c_t + c_f * \left(\left[\left(\frac{1}{2} * \rho(h) * S * V_{aircraft}^2 * C_{D0}\right) + \left(\frac{k * 2 * W^2}{\rho(h) * S * V_{aircraft}^2}\right) + (W * \sin(\theta))\right] * (c_a * V_{aircraft} + c_b) \right) \right) \quad (11)$$

Where V_{ground} is the resulting ground speed. Calculating the necessary aircraft heading to counter a wind speed and proceeding along a desired bearing to a destination, making use of the law of sines and the law of cosines, results in the equation (12)

$$V_{ground} = \sqrt{{V_{aircraft}}^2 + {V_{wind}}^2 - 2 * V_{aircraft} * V_{wind} * \cos\left(180 - \sigma - \left(\sin^{-1}\left(\frac{V_{wind} * \sin\sigma}{V_{aircraft}}\right)\right)\right)} \quad (12)$$

where:

$$\sigma = desired\ heading - wind\ heading \tag{13}$$

With the cost function presented in (11), it is possible to calculate the weight to go from one node to another in the graph considering parameters like wind speed, aircraft speed, operating cost, fuel cost, altitude difference and temperature. After defining the nodes, edges and the cost for every edge, the node diagram can be built. The algorithm was built with MATLAB/Simulink®, and it has a library enabling it to build a node diagram defining the nodes, edges and weights.

5 MODELING AND SIMULATION

To validate the algorithm, a series of models were developed. These models were integrated into a Simulink environment to simulate various flight scenarios. The six-degree-of-freedom (6DOF) aircraft model of a commercial aircraft model was developed. The model accepts inputs from the control surfaces, including the ailerons, tail, and rudder, as well as the throttle controls for both the left and right engines. Additionally, it accounts for the amount of fuel consumed and the speed and direction of the wind acting on the aircraft at any given moment. The outputs generated by the model include the velocities along the x, y, and z axes of the aircraft (denoted as u, v, and w), the angular velocities corresponding to rotations around these axes, and the Euler angles (φ, θ, ψ). Furthermore, the model provides translational speeds in relation to the north, east, and downward directions, along with the total fuel consumed during the flight. This proposed model is grounded in the work conducted by the Group of Aeronautical Research and Technology in Europe (GARTEUR), specifically referred to as the Research Civil Aircraft Model (RCAM) (Helmersson, A. et al, 1996). The aircraft parameters and initial conditions used in the simulation are listed in the Figure 8. The aircraft was modeled and trimmed with parameters similar to the Boeing 777-200 which features a wingspan of approximately 60.9 meters and a height of 18.5 meters. It has a maximum fuel capacity of 117,340 liters, enabling it to achieve a maximum takeoff weight (MTOW) of around 247,200 kg. The aircraft can accommodate up to 320 passengers, is designed for a maximum cruise speed of Mach 0.84 and has a maximum range of 5,240 nautical miles (9,700 km).

```
%Aircraft parameters
m = 220000 - delta_m;     %MTOW / Aicraft mass (kg) - Fuel Mass burned (kg)

cbar = 6.8;               %Mean Aerodynamic chord (m)
lt = 30;                  %Distance by AC of tail and body (m)
S = 427.80;               %Wing planform area (m²)
St = 92;                  %Tail planform area (m²)


Xcg = 0.23*cbar;          %x position of CoG in Fm (m)
Ycg = 0;                  %y position of CoG in Fm (m)
Zcg = 0.10*cbar;          %z position of CoG in Fm (m)


Xac = 0.12*cbar;          %x position of aerodynamic center in Fm (m)
Yac = 0;                  %y position of aerodynamic center in Fm (m)
Zac = 0;                  %z position of aerodynamic center in Fm (m)
```

```
%Engine constants
Xapt1 = 0;                %x position of engine 1 force in Fm (m)
Yapt1 = -8.94;            %y position of engine 1 force in Fm (m)
Zapt1 = -3;               %z position of engine 1 force in Fm (m)

Xapt2 = 0;                %x position of engine 2 force in Fm (m)
Yapt2 = 8.94;             %y position of engine 2 force in Fm (m)
Zapt2 = -3;               %z position of engine 2 force in Fm (m)

% Initial position and altitude

lon0 = deg2rad(-46.47206815021293); % GRU longitude Initial position
lat0 = deg2rad(-23.4305029894858);  % GRU latitude Initial position

h0 = 12000; % Initial Altitude [m] / 39370.079 [ft]

Vel = 249.9623; % Initial Speed [m/s] ~ 900 km/h ~ Mach Number = 0.8469
```

Figure 8: Aircraft Parameters and initial conditions.

The geodetic position model calculates the aircraft's position on the Earth's surface based on its translational speeds, allowing accurate trajectory tracking. The equations are based on some methods of computing the geodetic positions of points on a reference ellipsoid according to Vincenty's algorithm (Vincenty,1975).

Wind speed and direction data are obtained from real-time weather forecasts (Earth Null School, 2023) thereby ensuring that the algorithm functions with the most up-to-date information available. For the wind model, this data—comprising wind speed and direction—is manually compiled by sourcing information from weather forecast websites for each coordinate within the grid that the aircraft is projected to traverse. The model accepts as input the current positions of the aircraft, specified by latitude, longitude, and altitude, and subsequently outputs the wind speed and direction corresponding to the coordinates that are nearest to the provided input values.

Once the optimal trajectory has been defined, the aircraft must follow the path predetermined by the algorithm, which in turn returns as output a set of numbers corresponding to the waypoints or nodes or vertices of the grid that, if followed in the specified sequence, will lead to a path with the lowest possible cost. This series of numbers will serve as a reference for the closed loop that will control the aircraft's control surfaces, as shown in Figure 9.

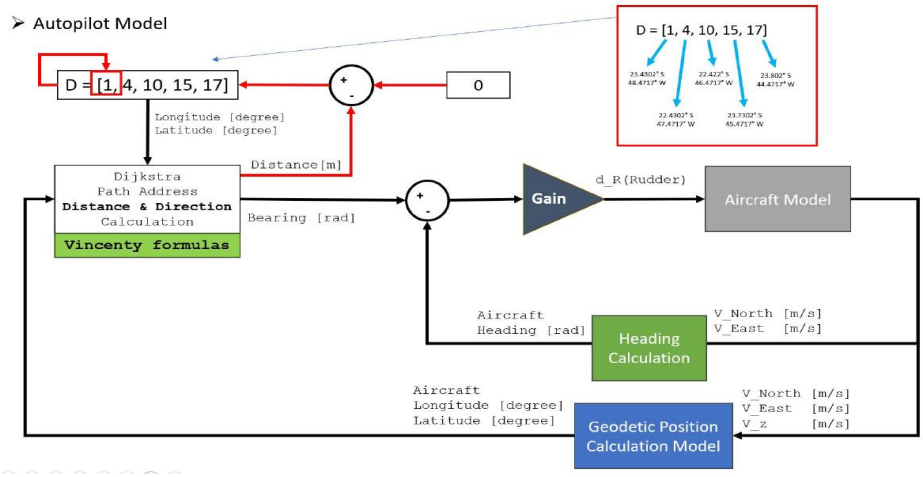

Figure 9: Autopilot Model.

The optimal trajectory array is represented by "D". For each node number in this array, there is a correspondent longitude, latitude and altitude. The distance between the current position of the aircraft and the next waypoint will be calculated using the inverse Vincenty method, which computes the geographical distance and azimuth (direction) between two given points. Thus, the aircraft heading will be adjusted in a way that its direction is aligned with the next waypoint direction. In this way, the difference between the aircraft heading and the bearing angle between the aircraft and the next waypoint will be proportional to the signal sent to the aircraft model input correspondent to the rudder/aileron control. The aircraft model will then return the translational speeds (V_N and V_E). With this information, it is possible to calculate the aircraft's geodesic position and its current heading, feeding back into the control loop. This loop will be performed until the distance between the aircraft and the next waypoint is zero. Once the distance is zero, the next waypoint on the list will be selected as reference.

6 RESULTS

For the proof of concept, a simulation was conducted to model a flight departing from Guarulhos International Airport (GRU/SBGR) and arriving at Cape Town Airport (CPT/FACT). The comprehensive Simulink model utilized for this simulation is presented in Figure 10.

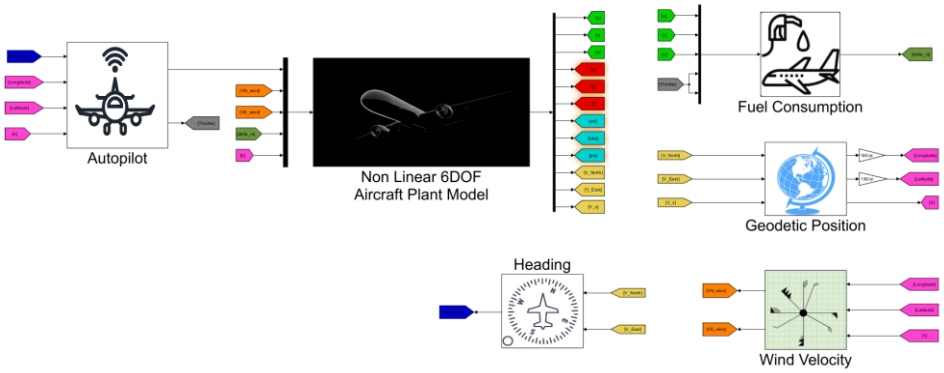

Figure 10: Simulink model.

The grid was constructed utilizing three distinct altitude levels in the vertical dimension, alongside eleven divisions in the horizontal plane extending both to the right and left, and six divisions in the horizontal direction leading to the endpoint. In the second layer of the grid, this wind data was integrated in a manner designed to facilitate a more expedient route for the aircraft to its destination. Figure 11 illustrates the path planner, which delineates the optimal trajectory for the aircraft, considering the wind data prior to the flight. It is evident that the algorithm recommended the path within the second layer, as anticipated.

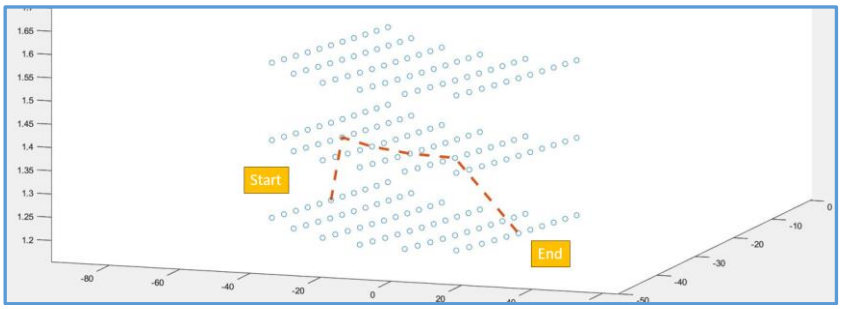

Figure 11: Path Planner Before Flight Simulation Showing the Optimal Path.

At the initial entry point, at Brazil southern coast near the city of Vitoria, the initial gross weight of the aircraft was 220,000 kg, at an altitude of 39,000ft and cruise Mach Number of 0.85. The simulations resulted in a trip time of 7h31m54s and a fuel consumption of 55,642 kg for the optimized trajectory. The trajectory undertaken by the aircraft for a conventional route, for the same initial conditions, which considered the great circle route between entry and exit waypoints within the AORRA airspace, the travel time was 7h41m56s and a fuel consumption of 56,894 kg which represented fuel savings of 1,252 kg or 2.2%. This finding suggests that optimizing flight paths by incorporating wind effects in both lateral and vertical profiles may result in substantial operational efficiencies.

7 CONCLUSION

The proposed algorithm for optimizing vertical and lateral tracking within flight management systems demonstrates significant potential for reducing fuel consumption and enhancing flight efficiency. Validation of the algorithm was conducted through the simulations of a South Atlantic route scenario, revealing its capacity to achieve potentially 2% reduction in fuel consumption relative to traditional flight planning methodologies. The results indicate that optimizing flight paths by incorporating wind effects can yield substantial operational efficiencies and contribute to the sustainability objectives of the aviation industry. Future research is suggested to concentrate on the integration of this algorithm into existing flight planning systems, as well as further validation in real-world contexts. Additionally, there is a critical need to automate the data retrieval process for wind speed and direction. Currently, the algorithm depends on manually sourced wind data, which can be both time-consuming and prone to inaccuracies. By incorporating automated data feeds from reliable meteorological sources, the algorithm can ensure operation with the most current and precise wind information available. This enhancement would also facilitate the use of grids with significantly higher resolution (i.e., increased columns and rows), a capability that is not feasible with manual data sourcing.

8 REFERENCES

International Civil Aviation Organization. (2011). **Follow-up on AORRA Airspace Implementation.** Twelfth Meeting of the Air Traffic Management/Aeronautical Information Management/Search and Rescue Sub-Group (ATM/AIM/SAR SG/12). Available at: https://www2023.icao.int/WACAF/Documents/Meetings/2011/atm_aim_sar_sg_12/docs/atmsg12_wp07_en.pdf

Ma J, Xiang P, Yao Q, Jiang Z, Huang J, Li H. **Optimizing aircraft route planning based on data-driven and physics-informed wind field predictions**. Mathematics. 2025;13(3):367. doi: https://doi.org/10.3390/math13030367.

Ramee, Coline & Kim, Junghyun & Deguignet, Marie & Justin, Cedric & Briceno, Simon & Mavris, Dimitri. (2020). **Aircraft Flight Plan Optimization with Dynamic Weather and Airspace Constraints**.

Legrand, Karine & Puechmorel, Stéphane & Delahaye, Daniel & Zhu, Yao. (2018). **Robust Aircraft Optimal Trajectory in the Presence of Wind**. IEEE Aerospace and Electronic Systems Magazine. 33. 10.1109/MAES.2018.170050.

Murrieta Mendoza, Alejandro & Botez, Ruxandra. (2014). **Lateral Navigation Optimization Considering Winds and Temperatures for Fixed Altitude Cruise using the Dijsktra's Algorithm.** ASME International Mechanical Engineering Congress and Exposition, Proceedings (IMECE). 1. 10.1115/IMECE2014-37570.

Ng, Hok & Sridhar, Banavar & Grabbe, Shon. (2014). **Optimizing Aircraft Trajectories with Multiple Cruise Altitudes in the Presence of Winds**. Journal of Aerospace Information Systems. 11. 35-47. 10.2514/1.I010084.

Christina Schilk & Peter Hecker, (2014). **Dynamic Route Optimization based on Adverse Weather Data**. Institute of Flight Guidance, Technical University Braunschweig, Braunschweig, Germany

Gagné, Jocelyn & Murrieta Mendoza, Alejandro & Botez, Ruxandra & Labour, Dominique. (2013). **New Method for Aircraft Fuel Saving using a Flight Management System and its Validation on the L-1011 Aircraft.**

David Knapp, Terry Jameson, Edward Measure, Andrew Butler, (2008). **Optimized Flight Routing Based on Weather Impacts Grids**. U.S. Army Research Laboratory, White Sands Missile Range, New Mexico

Vincenty, T. (1975). **Geodetic inverse solution between antipodal points**. Richard Rapp Geodetic Science Ohio State University. Available at: https://geographiclib.sourceforge.io/geodesic-papers/vincenty75b.pdf

Helmersson, A. et al. 1996. **Robust flight control design challenge, problem formulation and manual: The Research Civil Aircraft Model (RCAM).** GARTEUR/TP-088-03. Available at: https://garteur.org/wp-content/reports/FM/FM_AG-08_TP-088-3.pdf

Earth Null School. (n.d.). ***Earth Null School: A global map of wind, weather, and ocean conditions*.** Retrieved October 2023, Available at: https://earth.nullschool.net. Accessed on: 19 Nov. 2025.